Measurement of the ^{8}B solar neutrino flux with the KamLAND liquid scintillator detector

S. Abe,[1] K. Furuno,[1] A. Gando,[1] Y. Gando,[1] K. Ichimura,[1] H. Ikeda,[1] K. Inoue,[1,2] Y. Kibe,[1,*] W. Kimura,[1] Y. Kishimoto,[1] M. Koga,[1,2] Y. Minekawa,[1] T. Mitsui,[1] T. Morikawa,[1] N. Nagai,[1] K. Nakajima,[1] K. Nakamura,[1,2] M. Nakamura,[1] K. Narita,[1] I. Shimizu,[1] Y. Shimizu,[1] J. Shirai,[1] F. Suekane,[1] A. Suzuki,[1] H. Takahashi,[1] N. Takahashi,[1] Y. Takemoto,[1] K. Tamae,[1] H. Watanabe,[1] B. D. Xu,[1] H. Yabumoto,[1] E. Yonezawa,[1] H. Yoshida,[1] S. Yoshida,[1] S. Enomoto,[2,†] A. Kozlov,[2] H. Murayama,[2,3] C. Grant,[4] G. Keefer,[4,‡] D. McKee,[4,§] A. Piepke,[2,4] T. I. Banks,[3] T. Bloxham,[3] J. A. Detwiler,[3] S. J. Freedman,[2,3] B. K. Fujikawa,[2,3] K. Han,[3] R. Kadel,[3] T. O'Donnell,[3] H. M. Steiner,[3] L. A. Winslow,[3,‖] D. A. Dwyer,[5] C. Mauger,[5,¶] R. D. McKeown,[5] C. Zhang,[5] B. E. Berger,[6] C. E. Lane,[7] J. Maricic,[7] T. Miletic,[7,**] M. Batygov,[8,††] J. G. Learned,[8] S. Matsuno,[8] S. Pakvasa,[8] M. Sakai,[8] G. A. Horton-Smith,[2,9] A. Tang,[9] K. E. Downum,[10] G. Gratta,[10] K. Tolich,[10] Y. Efremenko,[2,11] Y. Kamyshkov,[11] O. Perevozchikov,[11,‡‡] H. J. Karwowski,[12] D. M. Markoff,[12] W. Tornow,[12] K. M. Heeger,[2,13] F. Piquemal,[14] J. -S. Ricol,[14] and M.P. Decowski[2,3,15]

(KamLAND Collaboration)

[1]*Research Center for Neutrino Science, Tohoku University, Sendai 980-8578, Japan*
[2]*Institute for the Physics and Mathematics of the Universe, Tokyo University, Kashiwa 277-8568, Japan*
[3]*Physics Department, University of California, Berkeley and Lawrence Berkeley National Laboratory, Berkeley, California 94720, USA*
[4]*Department of Physics and Astronomy, University of Alabama, Tuscaloosa, Alabama 35487, USA*
[5]*W. K. Kellogg Radiation Laboratory, California Institute of Technology, Pasadena, California 91125, USA*
[6]*Department of Physics, Colorado State University, Fort Collins, Colorado 80523, USA*
[7]*Physics Department, Drexel University, Philadelphia, Pennsylvania 19104, USA*
[8]*Department of Physics and Astronomy, University of Hawaii at Manoa, Honolulu, Hawaii 96822, USA*
[9]*Department of Physics, Kansas State University, Manhattan, Kansas 66506, USA*
[10]*Physics Department, Stanford University, Stanford, California 94305, USA*
[11]*Department of Physics and Astronomy, University of Tennessee, Knoxville, Tennessee 37996, USA*
[12]*Triangle Universities Nuclear Laboratory, Durham, North Carolina 27708, USA and Physics Departments at Duke University, North Carolina Central University, and the University of North Carolina at Chapel Hill*
[13]*Department of Physics, University of Wisconsin, Madison, Wisconsin 53706, USA*
[14]*CEN Bordeaux-Gradignan, IN2P3-CNRS and University Bordeaux I, F-33175 Gradignan Cedex, France*
[15]*Nikhef, Science Park, Amsterdam, Netherlands*

(Received 8 June 2011; published 13 September 2011)

We report a measurement of the neutrino-electron elastic scattering rate from ^{8}B solar neutrinos based on a 123 kton-day exposure of KamLAND. The background-subtracted electron recoil rate, above a 5.5-MeV analysis threshold is $1.49 \pm 0.14(\text{stat}) \pm 0.17(\text{syst})$ events per kton-day. Interpreted as due to a pure electron flavor flux with a ^{8}B neutrino spectrum, this corresponds to a spectrum integrated flux of $2.77 \pm 0.26(\text{stat}) \pm 0.32(\text{syst}) \times 10^{6}$ cm^{-2}s^{-1}. The analysis threshold is driven by ^{208}Tl present in the liquid scintillator, and the main source of systematic uncertainty is due to background from cosmogenic ^{11}Be. The measured rate is consistent with existing measurements and with standard solar model predictions which include matter-enhanced neutrino oscillation.

DOI: 10.1103/PhysRevC.84.035804 PACS number(s): 26.65.+t, 14.60.Pq, 13.15.+g

*Present address: Department of Physics, Tokyo Institute of Technology, Tokyo 152-8551, Japan.
†Jointly at: Center for Experimental Nuclear Physics and Astrophysics, University of Washington, Seattle, Washington 98195, USA.
‡Present address: Lawrence Livermore National Laboratory, Livermore, California 94550, USA.
§Present address: Department of Physics, Kansas State University, Manhattan, Kansas 66506, USA.
‖Present address: Department of Physics, Massachusetts Institute of Technology, Cambridge, MA 02139, USA.
¶Present address: Subatomic Physics Group, Los Alamos National Laboratory, Los Alamos, NM 87545, USA.
**Present address: Department of Physics and Astronomy, Rowan University, Glassboro, New Jersey 08028, USA.
††Present address: SNOLAB, Lively, ON P3Y 1N2, Canada.
‡‡Present address: Department of Physics, Louisiana State University, Baton Rouge, LA 70803 USA.

Neutrinos from ^{8}B β decay ($Q \sim 18$ MeV) dominate the high-energy portion of the solar neutrino spectrum and have been a crucial source for solar neutrino experiments. Such experiments, together with reactor antineutrino experiments, have established flavor change through large mixing angle (LMA) neutrino oscillation with matter effects, introduced by Mikheev, Smirnov, and Wolfenstein (MSW) [1,2], as a consistent resolution of the solar neutrino problem [3–10]. Measurements of neutrino-electron scattering using water-Cherenkov techniques have been achieved in a number of different detectors: Kamiokande [11,12], Super-Kamiokande [5,6,13], and the Sudbury Neutrino Observatory (SNO) [7–10]. An advantage of this detection technique is sensitivity to the neutrino direction of incidence, although analysis thresholds of $\sim$5 MeV are typically imposed. Recently, SNO has achieved a threshold of $\sim$3.5 MeV [10]. Liquid scintillator detectors may also be used to measure neutrino-electron elastic scattering; while insensitive to the neutrino direction, these detectors have better energy resolution and have the possibility of lower energy thresholds. A measurement with a threshold of $\sim$3.0 MeV, the lowest to date, has been reported by Borexino [14]. In this paper we report an independent, liquid-scintillator-based measurement of the ^{8}B flux with KamLAND.

The KamLAND detector consists of 1 kton of liquid scintillator (LS) confined in a 6.5-m-radius, 135-μm-thick, spherical balloon. The LS is 80% dodecane, 20% pseudocumene, and 1.36 ± 0.03 g/l of PPO; the density is 0.78 g/cm^3. The balloon is suspended in purified mineral oil within a 9-m-radius stainless steel sphere (SSS). The scintillation light is recorded by an array of 1879 photomultiplier tubes (PMTs) mounted on the inner surface of the SSS; 554 are reused 20-inch PMTs from Kamiokande, and the remainder are new 20-inch PMTs with the photo-cathode masked down to 17 inches. The 17-inch tubes have better timing and single-photoelectron (spe) resolution. A 3.2 kton, water-Cherenkov detector surrounds the SSS. It is used as a muon anticoincidence counter and as shielding against external γ rays and neutrons.

Event position (vertex) and energy are reconstructed based on the photon hit-time and charge distributions and a detector response model which is calibrated by periodically deploying radioactive sources: ^{203}Hg, ^{137}Cs, ^{68}Ge, ^{65}Zn, ^{60}Co, ^{241}Am^{9}Be, and ^{210}Po^{13}C. For the current analysis, the reconstruction omits the 20-inch PMTs due to their poorer timing and spe resolution; in this mode the energy resolution is $7\%/\sqrt{E(\mathrm{MeV})}$.

The signal of interest, neutrino-electron elastic scattering from ^{8}B solar neutrinos produces recoil electrons with reconstructed energy up to $\sim$20 MeV. We construct a *vertex*-χ^2 test to select electron-recoil-like events. The test compares the observed PMT charge and hit-time distributions as a function of the distance to the event to the expected distributions. The expected distributions and selection criteria were developed and calibrated based on source calibration data and muon-tagged β^-events from cosmogenic ^{12}B/^{12}N . The efficiency of the selection is 0.99 ± 0.01.

The analysis is carried out in *reconstructed* energy with a threshold of 5.5 MeV, which corresponds to a 5-MeV threshold in physical electron recoil energy. The threshold is chosen to reject background from ^{208}Tl($Q = 5.0$ MeV, $\tau_{1/2} = 3.05$ min) produced by residual ^{232}Th contamination present in the LS at a level of $(7.90 \pm 0.25) \times 10^{-17}$ g/g.

An energy-scale model was developed to convert physical energy to reconstructed energy. The model includes the linear response of the LS and particle-dependent nonlinearities such as scintillator quenching and Cherenkov light production. The energy scale is constrained by calibration data, tagged α particles from ^{214}Bi-^{214}Po/^{212}Bi-^{212}Po decays from residual ^{238}U/^{232}Th in the LS and high-energy β^- decays ($Q \sim$ 14 MeV) from cosmogenic ^{12}B/^{12}N .

The measurement reported here is restricted to data acquired before the KamLAND LS purification. The data were taken between April 2002 through April 2007 and correspond to 1432.1 days of run time. To reduce the external γ-ray background the fiducial volume (FV) is reduced to a 6-m-high, 3-m-radius cylinder centered at the detector center. This shape defines an optimal analysis volume that takes advantage of further shielding by the ultrapure LS from backgrounds coming from the cavern's rock walls and a large steel deck which caps the experiment. The FV fraction and systematic uncertainty are determined from short-lived muon spallation products, mainly ^{12}B($Q = 13.4$ MeV, $\tau_{1/2} = 20.2$ ms), which are assumed to be produced uniformly in the LS. The FV fraction is taken as the ratio of the number of spallation products that reconstruct inside the analysis cylinder to the number that reconstruct in the full LS volume. This fraction combined with the total LS volume in the balloon, which was measured directly during construction to be 1171 ± 25 m^3, gives a fiducial volume of 176.4 m^3 with an uncertainty of 3.1%. When all selection cuts, to be described, are applied the remaining exposure is 123 kton-days.

This paper focuses on neutrino-electron elastic scattering, $\nu + e^- \rightarrow \nu + e^-$ (ES) due to ^{8}B solar neutrinos. With 3.423×10^{32} e^- targets per kton of LS, we expect, including oscillation, 1.19 recoil events per kton-day from ^{8}B in the energy-region of interest (ROI) 5.5–20 MeV. In our calculation we adopt the standard solar model (SSM) of Serenelli *et al.* [16] which uses the solar abundances of Asplund *et al.* [17] (AGSS09). This predicts a total ^{8}B neutrino flux, independent of neutrino flavor, of $\Phi_{^8\mathrm{B}} = 4.85^{+0.58}_{-0.58} \times 10^6$ cm^{-2}s^{-1}. We use the ES cross section from Ref. [18], the ^{8}B-ν_e spectrum of Winter *et al.* [19], the oscillation parameters from the global analysis analysis in Ref. [4], and fold in the detector response. Elastic scattering from *hep* neutrinos and neutrino interactions on carbon in the LS are treated as a background and are discussed later in the paper. We note that the best choice of solar abundances to use in the SSM is an unresolved question. In AGSS09 the helioseismic discrepancy which emerged when the abundances of Asplund *et al.* [20] (AGS05) were adopted still persists, although it is not as severe. If the older, one-dimensional, solar abundance evaluation of Grevesse and Sauval [21] (GS98) is used, the SSM has excellent consistency with helioseismology and the predicted ^{8}B flux is $\Phi_{^8\mathrm{B}} = 5.88^{+0.65}_{-0.65} \times 10^6$ cm^{-2}s^{-1}. Assuming no sterile neutrinos, the total ^{8}B flux is directly observed in the SNO neutral current measurement to be $\Phi_{^8\mathrm{B}} = 5.140^{+0.197}_{-0.207} \times 10^6$ cm^{-2}s^{-1} [10].

TABLE I. Production rate of muon-spallation isotopes that dominate the background (in events per kton-day) [15]. *Nonbright* muons produce fewer than 7×10^5 p.e. in the PMT array.

Isotope	Q (MeV)	$\tau_{1/2}$ (s)	All muons	Nonbright muons
^{8}Li	16	0.84	15.6 ± 3.2	0.7 ± 0.4
^{8}B	18	0.77	10.7 ± 2.9	<0.006
^{11}Be	11.5	13.8	1.4 ± 0.3	0.27 ± 0.30

With the 5.5-MeV analysis threshold the background is dominated by decays of light isotopes produced by muon spallation. An in-depth study of muon activation at KamLAND can be found in Ref. [15]. A study of light isotope production shows that most (>80%) light isotope backgrounds are correlated with muons which produce more than 700 000 photoelectrons (p.e.) in the PMT array. We denote these as *bright* muons. The rate of bright muons is 0.037 Hz, while the total rate of muons passing through the LS is 0.198 ± 0.014 Hz. We apply a number of muon-related cuts to reduce these spallation backgrounds. All events within 200 ms of a preceding muon are rejected. This time veto of the full detector significantly reduces the background from ^{12}B/^{12}N. For nonbright muons, for which the muon tracking algorithm converged successfully—well-tracked muons—a 5-s veto is applied within a 3-m-radius cylinder around the muon track. Using the ^{12}B/^{12}N candidates we determine that $97 \pm 6\%$ of spallation products are contained within this cylinder. For bright muons and any muon with a poorly reconstructed track, the 5-s veto is applied to the full detector. These cuts reduce the exposure by $62.4 \pm 0.1\%$ to a total exposure of 123 kton-days. The spallation background events remaining after these cuts are expected to come mainly from long lived ($\tau > 1$ s) spallation products, ^{11}Be, ^{8}Li, ^{8}B. The total production rates of these key isotopes [15], along with the rates correlated to nonbright muons, are summarized in Table I.

The next-largest background is from external γ rays which are primarily the result of (n,γ) reactions in the surrounding rock cavern and stainless steel detector elements. The external γ-ray spectrum has peaks in reconstructed energy at 8.5 and 10 MeV from stainless steel and at 5.5 MeV from neutron capture on silicon in the rock. The cylindrical fiducial volume was chosen to optimize the shielding for a given exposure. The closest points to the cylindrical external rock cavity are at the balloon equator, while the closest stainless steel component is a balloon support structure at the top of the detector. A GEANT4-based Monte Carlo [22,23], including the full detector and shielding geometry, simulated the effect of LS self-shielding from sources in the stainless steel and the rock. The simulation indicates that γs are attenuated approximately exponentially with an attenuation length of 53.0 ± 0.1 cm for rock and 50.7 ± 0.1 cm for stainless steel. Using data within a 6-m-radius volume, we observe attenuation lengths for γs from the rock and stainless steel of 59.0 ± 1.9 cm and 54.9 ± 1.9 cm, respectively. We estimate 25.2 ± 12.6 electron-recoil-like events from external γ rays in the ROI within the cylindrical fiducial volume. The uncertainty in the estimate comes from the difference in the observed and simulated attenuation lengths.

As remarked earlier, events from *hep* solar neutrinos and solar neutrino interactions on carbon are treated as a background. Using the SSM with AGSS09 and the *hep* spectrum from Ref. [24], we estimate, including oscillation, 0.6 ± 0.1 electron recoil events from *hep* neutrinos in the ROI. In our calculation we use the ES cross section, neutrino oscillation parameters, and detector response as was done for the ^{8}B ES calculation. The uncertainty is dominated by the

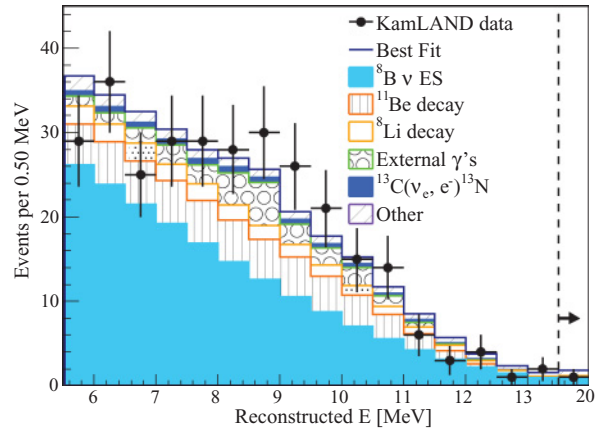

FIG. 1. (Color) Energy spectrum of ^{8}B candidates with the best-fit spectrum and background components from the unbinned energy and rate analysis. The histograms display the results in bins of 0.5 MeV except for the last bin which due to limited statistics extends from 13.5 to 20 MeV.

TABLE II. Estimated background contributions for the full exposure and after all cuts. The shorter lived spallation products ^{12}B, ^{12}N, ^{9}C, ^{9}Li, and ^{8}He are also considered and their contributions are summarized by "spallation other."

Background	Counts
Spallation ^{11}Be	89.1 ± 19.1
Spallation ^{8}Li	20.5 ± 4.0
Spallation ^{8}B	11.0 ± 3.0
Spallation other	0.4 ± 0.6
External γ rays	25.2 ± 12.6
^{8}B CC on ^{13}C GND	5.8 ± 1.4
Reactor $\bar{\nu}_e$	1.6 ± 0.1
^{8}B CC on ^{13}C 3.51 MeV	1.1 ± 0.4
hep ES	0.6 ± 0.1
Atmospheric ν	2.0 ± 2.0
Total	157.3 ± 23.6

TABLE III. The systematic uncertainties associated with the unbinned fit to the energy spectrum of the ^{8}B candidates. The detection efficiency is dominated by our fiducial volume uncertainty.

Source	Uncertainty (%)
^{11}Be	10.8
^{8}Li and ^{8}B	3.3
External γ rays	6.8
Other backgrounds	1.1
Detection efficiency	6.3
Energy scale	0.8

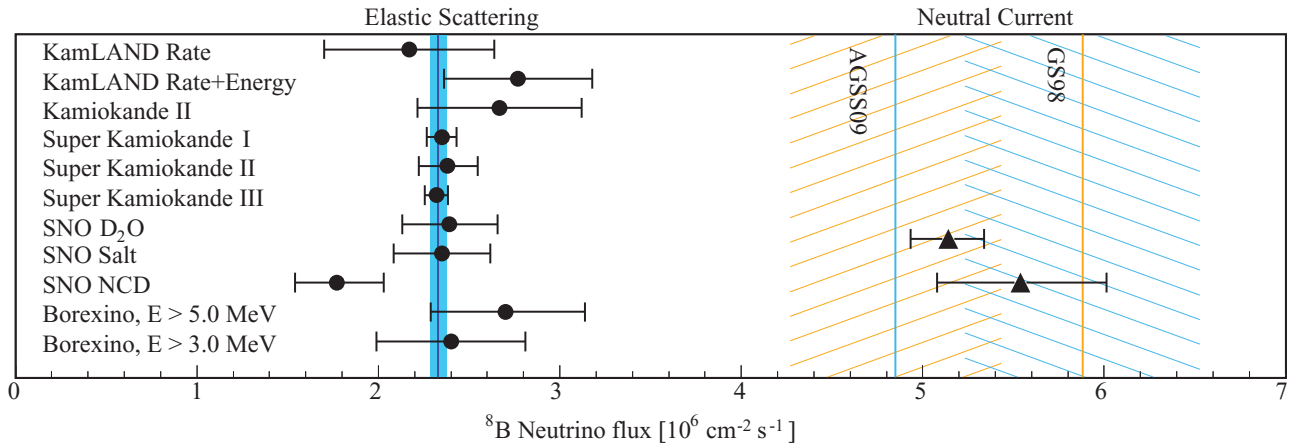

FIG. 2. (Color) Summary of measurements of the ^{8}B flux using neutrino-electron scattering: this work KamLAND, Kamiokande II [11,12], Super Kamiokande I [5], Super Kamiokande II [6], Super Kamiokande III [13], SNO D_2O [7,10], SNO Salt [8,10], SNO NCD [9], and Borexino [14]. The SNO neutral current measurements [9,10] are shown for reference with closed triangles.

difference in the flux prediction of the SSM with the AGSS09 versus with the GS98 solar abundances.

There are 4.30×10^{31} carbon nuclei per kton of LS if we assume a natural ^{13}C of 1.10%. Using the cross sections calculated in Ref. [25], we find the largest ν_e-C scattering background contribution to be from charged current (CC) scattering, $^{13}\mathrm{C}+\nu_e \rightarrow {}^{13}\mathrm{N}+e^-$ from ^{8}B. We estimate, including oscillation, that scattering to the ground state of ^{13}N produces 5.8 ± 1.4 events in the ROI; and scattering to the 3.51 MeV first excited state, which decays by proton emission, contributes 1.1 ± 0.4 electron-recoil-like events in the ROI. In this estimate, an additional uncertainty of 30% on the cross section is included. The contribution from higher states of ^{13}N, neutral current (NC) scattering by ^{8}B-ν and $hep-\nu$ NC, and CC interactions on carbon is estimated to be fewer than 0.13 events in the ROI and is considered negligible given the other backgrounds. These calculations use the same solar-ν fluxes, spectra, detector response, and oscillation parameters as before. The effect of using the oscillation parameters from the global analyses in Refs. [13,26] were investigated but do not change the result due to the large flux and cross section uncertainties.

In addition to these neutrino interactions, we expect a small background from atmospheric neutrino interactions. Assuming a flat spectrum, we use the candidate events in the range of 20 to 35 MeV to extrapolate the atmospheric neutrino contribution in the signal region and find 2.0 ± 2.0 events.

A background from positrons from inverse β decay induced by reactor antineutrinos is tagged by coincidence with delayed neutron capture γ rays. The mean capture time in KamLAND is $\sim$207 μs. The tagging cuts are a delayed energy cut, $2.04\,\mathrm{MeV} < E < 2.82\,\mathrm{MeV}$, to select the 2.2-MeV n-p capture γ; a timing cut, $0.5\,\mu\mathrm{s} < \Delta T < 660\,\mu\mathrm{s}$; and a position cut, $\Delta R < 1.6$ m. ΔT and ΔR refer respectively to the time and distance between the prompt positron and delayed capture γ. The tagging efficiency is 0.940 ± 0.006. The reactor antineutrino flux at KamLAND is dominated by Japanese power reactors, we calculate the flux and spectrum using data provided by the Japanese power companies and a simplified reactor model [27]. The residual background is 1.6 ± 0.1, where the uncertainty in the neutrino oscillation parameters is included. The total background, broken down in Table II, is estimated to be 157.3 ± 23.6 events. While ^{8}Li has the largest production rate, ^{11}Be, due to its long half-life ($\tau_{1/2} = 13.8$ s), is the largest contribution to the total background.

After applying all the cuts, 299 electron recoil candidates are found in the ROI in the 123 kton-day exposure. Subtracting the 157.3 ± 23.6 background events gives a ^{8}B rate of $1.16 \pm 0.14(\mathrm{stat}) \pm 0.21(\mathrm{syst})$ events per kton-day which is consistent with our prediction including neutrino oscillation. If we neglect neutrino oscillation, assume a pure ν_e flux, and correct for the 5.5-MeV threshold, the measured rate corresponds to a spectrum integrated flux of $\Phi_{\mathrm{ES}} = 2.17 \pm 0.26(\mathrm{stat}) \pm 0.39(\mathrm{syst}) \times 10^6\ \mathrm{cm}^{-2}\mathrm{s}^{-1}$.

A second analysis of this data uses an unbinned maximum likelihood fit to the ^{8}B candidate energy spectrum. The normalization of the individual backgrounds are allowed to vary but are constrained by a penalty to the expected value. The best-fit rate is $1.49 \pm 0.14(\mathrm{stat}) \pm 0.17(\mathrm{syst})$ events per kton-day, with a goodness-of-fit of 49%. Once again assuming a pure ν_e flux, this corresponds to a spectrum integrated flux of $\Phi_{\mathrm{ES}} = 2.77 \pm 0.26(\mathrm{stat}) \pm 0.32(\mathrm{syst}) \times 10^6\ \mathrm{cm}^{-2}\mathrm{s}^{-1}$. Figure 1 shows the energy spectrum of the candidate events with the best-fit solar neutrino and background spectra. This analysis does not include the small change in the shape of the neutrino spectra due to oscillation. Including this effect does not significantly change the best-fit rate, $\Phi_{\mathrm{ES}} = 2.74 \pm 0.26(\mathrm{stat}) \pm 0.32(\mathrm{syst}) \times 10^6\ \mathrm{cm}^{-2}\mathrm{s}^{-1}$, with a goodness of fit of 57%.

The KamLAND result is compared to other measurements of the total ^{8}B flux through neutrino-electron elastic scattering in Fig. 2. For this comparison the reported statistical and systematic errors are added in quadrature. The mean of the experiments, weighted by their uncertainties, is $\Phi_{\mathrm{ES}} = 2.33 \pm 0.05 \times 10^6\ \mathrm{cm}^{-2}\mathrm{s}^{-1}$. This is dominated by the very precise Super-Kamiokande water-Cherenkov measurement (Table III). The reduced χ^2/NDF is 6.6/8, where the KamLAND rate+energy result and the Borexino $E > 3$ MeV result are used in the calculation.

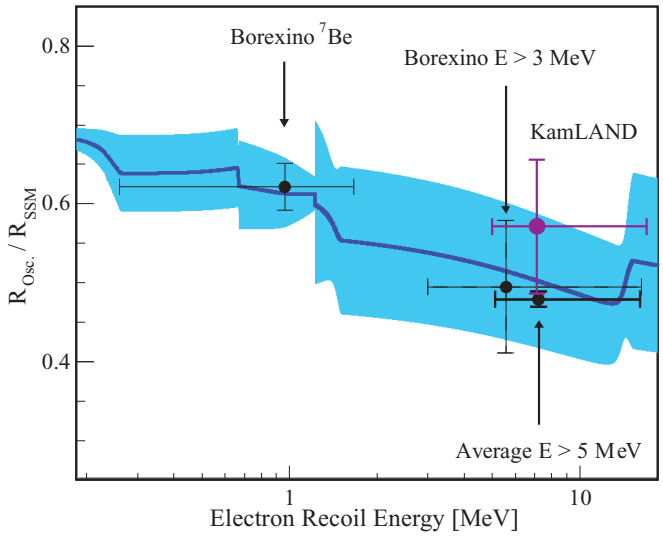

FIG. 3. (Color) Ratio of the measured (threshold corrected) solar neutrino-electron elastic-scattering rate and that predicted by the AGSS09-SSM as a function of energy (data points). The average of the water-Cherenkov detector results above 5 MeV is shown. The horizontal error bars indicate the range of energy over which the flux was measured. The central value indicates the flux averaged energy for that range. The solid curve (and $\pm$ 1σ band) shows the ratio of AGSS09 with neutrino oscillation included to the prediction without oscillation. The discontinuities in the prediction arise as different neutrino sources become significant, the large uncertainty in the CNO neutrinos is evident at $\sim$1.2 MeV.

A key prediction of the LMA-MSW solution to the solar neutrino problem is the expected transition from matter-dominated to vacuum-dominated oscillations, depending on the neutrino energy and the region of the solar interior probed by the neutrinos as they journey out of the sun. A general feature is that the survival probability, defined as the ratio of the oscillated ν_e flux to the unoscillated flux, tends to increase with decreasing solar neutrino energy. This effect is the result of neutrino species (^{8}B, ^{7}Be, pp, etc.) either moving off or being produced in a region not satisfying the MSW resonance condition. These neutrinos are then described by vacuum oscillation. The curve in Fig. 3 shows the ratio of the expected neutrino-electron elastic-scattering rates with and without oscillation calculated using the AGSS09-SSM. The data points are the survival probabilities deduced, relative to the SSM prediction, from neutrino-electron elastic-scattering measurements at Borexino, KamLAND, and the combined water-Cherenkov experiments. The Borexino ^{8}B measurement with a 3.0-MeV threshold [14] and the ^{7}Be flux measurement [28,29] are consistent with the LMA-MSW prediction. The measurements are not yet precise enough to resolve the issue of solar abundances.

This letter reports a measurement of the ^{8}B solar neutrino flux measured through neutrino-electron elastic scattering in the KamLAND LS. Our result is in good agreement with existing measurements from both water-Cherenkov and liquid-scintillator-based detectors. In the data set presented, ^{208}Tl background limits the KamLAND analysis threshold to 5.5 MeV. We expect to achieve a lower threshold in a future analysis of data taken after purification of the KamLAND LS.

The KamLAND experiment is supported by a Grant-in-Aid for Specially Promoted Research under Grant No. 16002002 of the Japanese Ministry of Education, Culture, Sports, Science and Technology; the World Premier International Research Center Initiative (WPI Initiative), MEXT, Japan; and under the US Department of Energy (DOE) Grants No. DE-FG03-00ER41138, No. DE-AC02-05CH11231, and No. DE-FG02-01ER41166, as well as other DOE grants to individual institutions. The reactor data are provided by courtesy of the following electric associations in Japan: Hokkaido, Tohoku, Tokyo, Hokuriku, Chubu, Kansai, Chugoku, Shikoku, and Kyushu Electric Power Companies, Japan Atomic Power Co., and Japan Atomic Energy Agency. The Kamioka Mining and Smelting Company provided service for activities in the mine.

[1] S. P. Mikheev and A. Y. Smirnov, Sov. J. Nucl. Phys. **42**, 913 (1985).
[2] L. Wolfenstein, Phys. Rev. D **17**, 2369 (1978).
[3] K. Nakamura *et al.* (Particle Data Group Collaboration), J. Phys. G **37**, 075021 (2010).
[4] S. Abe *et al.* (KamLAND Collaboration), Phys. Rev. Lett. **100**, 221803 (2008).
[5] S. Fukuda *et al.* (Super-Kamiokande Collaboration), Phys. Lett. B **539**, 179 (2002).
[6] J. P. Cravens *et al.* (Super-Kamiokande Collaboration), Phys. Rev. D **78**, 032002 (2008).
[7] B. Aharmim *et al.* (SNO Collaboration), Phys. Rev. C **75**, 045502 (2007).
[8] B. Aharmim *et al.* (SNO Collaboration), Phys. Rev. C **72**, 055502 (2005).
[9] B. Aharmim *et al.* (SNO Collaboration), Phys. Rev. Lett. **101**, 111301 (2008).
[10] B. Aharmim *et al.* (SNO Collaboration), Phys. Rev. C **81**, 055504 (2010).
[11] K. S. Hirata *et al.* (Kamiokande-II Collaboration), Phys. Rev. Lett. **63**, 16 (1989).
[12] K. S. Hirata *et al.* (Kamiokande-II Collaboration), Phys. Rev. D **44**, 2241 (1991).
[13] K. Abe *et al.* (Super-Kamiokande Collaboration), Phys. Rev. D **83**, 052010 (2011).
[14] G. Bellini *et al.* (Borexino Collaboration), Phys. Rev. D **82**, 033006 (2010).
[15] S. Abe *et al.* (KamLAND Collaboration), Phys. Rev. C **81**, 025807 (2010).
[16] A. Serenelli, S. Basu, J. W. Ferguson, and M. Asplund, Astrophys. J. Lett. **705** (2009).
[17] M. Asplund, N. Grevesse, A. J. Sauval, and P. Scott, Annu. Rev. Astron. Astrophys. **47**, 481 (2009).
[18] J. N. Bahcall, M. Kamionkowski, and A. Sirlin, Phys. Rev. D **51**, 6146 (1995).
[19] W. T. Winter, S. J. Freedman, K. E. Rehm, and J. P. Schiffer, Phys. Rev. C **73**, 025503 (2006).

[20] M. Asplund, N. Grevesse, and A. Sauval, Nuclear Physics A **777**, 1 (2006).
[21] N. Grevesse and A. J. Sauval, Space Sci. Rev. **85**, 161 (1998).
[22] S. Agostinelli *et al.* (GEANT4 Collaboration), Nucl. Instrum. Methods A **506**, 250 (2003).
[23] J. Allison *et al.*, IEEE Trans. Nucl. Sci. **53**, 270 (2006).
[24] J. N. Bahcall and R. K. Ulrich, Rev. Mod. Phys. **60**, 297 (1988).
[25] M. Fukugita, Y. Kohyama, K. Kubodera, and T. Kuramoto, Phys. Rev. C **41**, 1359 (1990).
[26] A. Gando *et al.* (KamLAND Collaboration), Phys. Rev. D **83**, 052002 (2011).
[27] K. Nakajima *et al.*, Nucl. Instrum. Methods A **569**, 837 (2006).
[28] G. Bellini *et al.* (Borexino Collaboration) (2011), arXiv:1104.1816 [hep-ex].
[29] C. Arpesella *et al.* (Borexino Collaboration), Phys. Rev. Lett. **101**, 091302 (2008).